Inhibition of mitochondrial fission protects podocytes from albumin-induced cell damage in diabetic kidney disease

Makoto Tagaya,[1] Shinji Kume,[1] Mako Yasuda-Yamahara,[1] Shogo Kuwagata,[1] Kosuke Yamahara,[1] Naoko Takeda,[1] Yuki Tanaka,[1] Masami Chin-Kanasaki,[1] Yuki Nakae,[2] Hideki Yokoi,[3] Masashi Mukoyama,[4] Naotada Ishihara,[5] Masatoshi Nomura,[6] Shin-ichi Araki[1] and Hiroshi Maegawa[1]

[1]Department of Medicine, Shiga University of Medical Science, Tsukinowa-cho, Otsu, Shiga 520-2192, Japan.
[2]Departments of Stem Cell Biology and Regenerative Medicine, Shiga University of Medical Science, Tsukinowa-cho, Otsu, Shiga 520-2192, Japan.
[3]Department of Nephrology, Graduate School of Medicine, Kyoto University, 54 Shogoin Kawahara-cho, Sakyo-ku, Kyoto 606-8507 Japan.
[4]Department of Nephrology, Graduate School of Medical Sciences, Kumamoto University, 1-1-1 Honjo, Chuo-ku, Kumamoto, Kumamoto 860-8556, Japan.
[5]Department of Biological Sciences, Graduate School of Science, Osaka University, 1-1 Machikaneyama, Toyonaka 560-0043, Japan.
[6]Department of Endocrinology and Metabolism, Kurume University School of Medicine, 67 Asahi-machi, Kurume 830-0011, Japan.

Corresponding authors
Shinji Kume, M.D., Ph.D. & Shin-ichi Araki, M.D., Ph.D.
Department of Medicine, Shiga University of Medical Science
Tsukinowa-cho, Otsu, Shiga 520-2192, Japan.
TEL: +81-775-48-2222
FAX: +81-775-43-3858
E-mail (S. Kume): skume@belle.shiga-med.ac.jp
E-mail (S-i. Araki): araki@belle.shiga-med.ac.jp

Word count: 3,930
Character count: 28,621

ABSTRACT

Aims. Identifying the mechanisms that underlie progression from endothelial damage to podocyte damage, which leads to massive proteinuria, is an urgent issue that must be clarified to improve renal outcome in diabetic kidney disease (DKD). We aimed to examine the role of dynamin-related protein 1 (Drp1)-mediated regulation of mitochondrial fission in podocytes in the pathogenesis of massive proteinuria in DKD.

Methods. Diabetes- or albuminuria-associated changes in mitochondrial morphology in podocytes were examined by electron microscopy. The effects of albumin and other diabetes-related stimuli, including high glucose (HG), on mitochondrial morphology were examined in cultured podocytes. The role of Drp1 in podocyte damage was examined using diabetic podocyte-specific Drp1-deficient mice treated with neuraminidase, which removes endothelial glycocalyx.

Results. Neuraminidase-induced removal of glomerular endothelial glycocalyx in nondiabetic mice led to microalbuminuria without podocyte damage, accompanied by reduced Drp1 expression and mitochondrial elongation in podocytes. In contrast, streptozotocin-induced diabetes significantly exacerbated neuraminidase-induced podocyte damage and albuminuria, and was accompanied by increased Drp1 expression and enhanced mitochondrial fission in podocytes. Cell culture experiments showed that albumin stimulation decreased Drp1 expression and elongated mitochondria, although HG inhibited albumin-associated changes in mitochondrial dynamics, resulting in apoptosis. Podocyte-specific Drp1-deficiency in mice prevented diabetes-related exacerbation of podocyte damage and neuraminidase-induced development of albuminuria. Endothelial dysfunction-induced albumin exposure is cytotoxic to podocytes. Inhibition of mitochondrial fission in podocytes is a cytoprotective mechanism against albumin stimulation, which is impaired under diabetic condition. Inhibition of mitochondrial fission in podocytes may represent a new therapeutic strategy for massive proteinuria in DKD.

KEY WORDS: Diabetic kidney disease, podocyte, albuminuria, mitochondrial fission, Drp1

1. INTRODUCTION

Massive albuminuria leads to poor renal prognosis in patients with diabetic kidney disease (DKD) [1, 2]. The pathogenesis of DKD is therefore an urgent issue that must be clarified. The glomerular filtration barrier, which prevents albumin leakage, consists of three components: endothelium, glomerular basement membrane, and podocytes. Endothelial cell damage is considered the primary event in development of DKD [3, 4], and subsequent podocyte damage is involved in the development of massive proteinuria in DKD [5, 6]. Therefore, identifying the underlying mechanisms of progression from endothelial cell to podocyte damage should contribute to development of novel therapies for preventing the progression of albuminuria stage in DKD.

Glomerular endothelium is the initial gatekeeper of glomerular filtration barrier function, and therefore its injury causes albuminuria [7-9]. It is well established that albumin filtered from the glomerular barrier is reabsorbed by proximal tubular cells, leading to tubular cell damage as albuminuria increases [10, 11]. Similarly, accumulating evidence indicates that podocytes also reabsorb albumin that passes from glomerular endothelial cells and the glomerular basement membrane, and that leaked albumin injures podocytes, resulting in massive albuminuria [12-15]. Therefore, elucidation of the molecular mechanisms underlying albumin-induced podocyte damage may contribute to improved understanding of the pathogenesis of progression to massive albuminuria in kidney diseases that begin with endothelial damage.

Cells have evolved several stress-induced mechanisms for maintaining homeostasis under various stress conditions [16, 17]. Among them, we recently reported that the autophagy machinery, an intracellular degradation system that maintains cellular homeostasis under stress conditions, is responsible for maintaining the function and survival of podocytes exposed to albuminuria, and that insufficient autophagy exacerbated albumin-induced podocyte damage and increased albuminuria in animals with DKD [12]. These observations suggested that podocytes possess several homeostatic mechanisms that confer protection from albumin-induced cytotoxicity, and that disruption of these mechanisms is involved in the progression to massive albuminuria. However, the complete picture of the intracellular stress response mechanisms in podocytes that are designed to cope with albumin exposure remains unclear.

Mitochondria are important organelles that maintain intracellular ATP production, and mitochondrial abnormalities have recently been reported to be associated with podocyte damage in DKD [18, 19]. Mitochondria maintain their function via continual mitochondrial dynamics, which involve several key players [20]. Mitochondrial fission is primarily regulated by mitochondrial fission factor (Mff) and

dynamin-related protein 1 (Drp1), and mitochondrial fusion is regulated by optic atrophy 1 (Opa1) and mitofusins (Mfn) [20]. Increasing evidence has shown that aberrant mitochondrial dynamics are involved in the pathogenesis of several metabolic diseases [21, 22]. However, the role of mitochondrial dynamics in podocytes exposed to albuminuria in DKD remains incompletely understood.

In this study, we examined the role of mitochondrial dynamics in albumin-induced podocyte damage in DKD. To conclude it, we used podocyte-specific Drp1-deficient mice (Podo-*Drp1*$^{-/-}$), which provided insight into the role of podocyte-specific mitochondrial dynamics in DKD.

2. METHODS

2-1. Animal experiments

All animal handling and experimentation were conducted according to the guidelines of the Research Center for Animal Life Science at Shiga University of Medical Science. All experimental protocols were approved by the Gene Recombination Experiment Safety Committee (No.2-60) and the Research Center for Animal Life Science at Shiga University of Medical Science (No.2018-6-11 and 2021-5-11). The animals were housed in ventilated cages in specific pathogen-free (SPF) condition under a 12 h, light–dark cycle with free access to chow and water at the Research Center for Animal Life Science at Shiga University of Medical Science.

Diabetes was induced in male 8-week-old wild type C57BL/6J mice by intraperitoneal injection of 55 mg/kg/day streptozotocin (STZ) (Nacalai Tesque, Kyoto, Japan) dissolved in citrate buffer (pH 4.5) for 5 consecutive days [23]. At 3 weeks after STZ injection, mice with blood glucose >250 mg/dl were considered diabetic. Nondiabetic control mice were injected with citrate buffer alone. Male mice were used in all experiments. Urine samples were collected at 3 and 12 weeks after injection using metabolic cages. At 12 weeks after injection, mice were euthanized (75 mg/kg sodium pentobarbital i.p.) and perfused with phosphate-buffered saline following ventricular puncture which were conducted in the Research Center for Animal Life Science at Shiga University of Medical Science. Finally, mice were perfused with fixative buffer (4% paraformaldehyde in 0.1M phosphate buffer), and renal samples were collected and embedded in paraffin. The animal number used in this study was described in figure legends.

Neuraminidase removes glycocalyx on the vascular endothelial cell surface, and resultantly it can induce a transient mild albuminuria in mice [12, 24, 25]. In our previous

report on this model, we have shown that the glycocalyx temporarily disappears after 1-2 days of the treatment and is recovered by day 3 [12]. Thus, in this study, neuraminidase was administered in diabetic and nondiabetic male wild type at 3 weeks after administration of STZ or citrate buffer vehicle, respectively. Neuraminidase, a *Vibrio cholerae* Type III neuroaminidase from Sigma-Aldrich, is supplied in saline at pH 5.5 with 4 mM $CaCl_2$. The concentration was adjusted so that 3 mU/gBW could be administered in 100 μl of solution. Neuraminidase solution or vehicle was administered through the tail vein.

Next, urine samples were collected at days 1 or 3 following neuraminidase injection. After urine collection, mice were sacrificed and kidney tissues were paraffin-embedded as described above. A portion of kidney tissue samples were fixed for electron microscopy.

Podocyte-specific Drp1-deficient mice (Podo-$Drp1^{-/-}$) were generated using the Cre-LoxP system by breeding Drp1-flox ($Drp1^{f/f}$) mice [26] with tamoxifen-inducible podocyte-specific Cre^{ERT2} mice on a C57BL/6 background [27]. Eight-week-old male mice carrying podocin-Cre^{ERT2} were administered tamoxifen at 150 mg/kg/day for 5 consecutive days [28]. At 2 weeks after administration of tamoxifen, STZ or citrate buffer was administered as described above. After an additional 3 weeks, neuraminidase was administered and urine and kidney samples were collected as described above. In all animal experiments, albuminuria levels and decreased podocyte number were assessed as primary outcomes.

2-2. Blood and urinary analyses

Blood glucose concentrations were measured using GDH-PQQ glucose test strips (Glutest Sensor, Sanwa Kagaku, Nagoya, Japan). Urinary albumin excretion was measured using an Albumin Fluorometric Assay Kit (BioVision, Milpitas, CA, USA). Urinary albumin excretion was evaluated as daily excretion.

2-3. Histological analyses

Histological analyses were performed as previously reported [12]. Briefly, fixed paraffin-embedded kidneys were sectioned (3-mm thickness) and stained with antibodies against WT1 (sc-393498, 1:200, Santa Cruz Biotechnology, Dallas, TX, USA), Drp1 (ab56788, 1:200, Abcam, Cambridge, UK), and Isolectin GS-IB4 (I21413, 1:300, Invitrogen,

Eugene, OR, USA) for immunofluorescence analysis. Immunofluorescence analysis was conducted using a confocal laser scanning microscope (Leica, TCS SP8X). To determine podocyte number per glomerulus, WT1-positive cell number was counted in over 20 glomeruli per group. The glomerular area was measured in at least 10 glomeruli with either vascular or urinary poles in the renal cortex region of the kidney sections in each group using the ImageJ (Image Processing and Analysis in Java). Electron microscopic analyses were performed using JSM-7505FA (JEOL, Tokyo, Japan) and H-7500 (Hitachi, Tokyo, Japan) electron microscopes. Mitochondrial structure in podocytes was assessed by transmission electron microscopic examination of at least 30 mitochondria per group at magnification of ×20,000.

2-4. Cell culture

Conditionally immortalized human podocytes were a gift from Moin A. Saleem (Bristol Royal Hospital for Children, Bristol) [29]. The cells were cultured in RPMI-1640 supplemented with 10% heat-inactivated FBS, 100 U/ml penicillin, 0.1 mg/ml streptomycin, insulin, transferrin, and selenite in a humidified 5% (v/v) CO_2 atmosphere at 37°C under no mycoplasma contamination. These cells proliferate at 33°C. After transfer to 37°C, they enter growth arrest and express markers of differentiated podocytes *in vivo*. Expression of nephrin was confirmed in the differentiated podocytes used in this study. Cells were recovered and stained on days 10–14. Differentiated cells were preincubated with high glucose (500 mg/dL), transforming growth factor β (TGF-β, 10 ng/ml), tumor necrosis factor-α (TNF-α, 20 ng/μl), angiotensin II (Ang-II, 0.2 μM), mannitol (30 mM), or normal culture medium alone for 20 h. After preincubation, albumin fraction V (from bovine serum) was mixed with RPMI-1640 at 20 g/dl and medium containing the various stimulants to adjust the final albumin concentration to 5 g/dl. Podocytes were incubated for the specified times, and subjected to various analyses as follows. Apoptosis and ATP contents were assessed as a primary and a secondary outcome, respectively.

2-5. Mitochondrial staining

Differentiated podocytes were observed under a confocal laser scanning microscope (Olympus, FV1000-D) by replacing the culture medium with a solution containing MitoTracker Red (Invitrogen, Eugene, OR, USA) at ratio of 1:1000. The major axis of over 100 mitochondria per group was measured to determine mitochondrial length.

2-6. Western blot analysis

Protein samples were prepared from differentiated podocytes [30]. For western blot analysis, proteins were resolved by SDS-PAGE and transferred to nitrocellulose membranes. Membranes were incubated with antibodies against cleaved caspase 3 (Asp175) (Cell Signaling Technology, Danvers, MA, USA), Drp1 (Novus Biologicals, Littleton, CO, USA), or β-actin (Sigma-Aldrich, St. Louis, MO, USA). After additional washing, membranes were incubated with horseradish peroxidase-conjugated secondary antibodies before chemiluminescence detection.

2-7. ATP content

ATP concentration in cultured podocytes was measured using an intracellular ATP assay kit (Toyo Ink Group, Tokyo, Japan) and was evaluated per cell number.

2.8 Retrovirus-mediated gene transfer

HEK293T cells were transfected with p-BABE (Drp1K38A) (Addgene, Watertown, MA, USA) and p-BABE (empty) using Lipofectamine 3000 reagent (Thermo Fisher Scientific, Waltham, MA, USA) in accordance with the manufacturer's protocol. At 24 h after transfection, medium containing retrovirus was collected, centrifuged, and transferred to human podocytes. The cells were treated with puromycin (2.5 μg/ml) for 24 h to select for infected cells [31].

2.9 Quantitative Real-Time PCR

Total RNA was isolated from cultured podocytes according to the TRIzol protocol (Invitrogen, Carlsbad, CA, USA). cDNA was synthesized using reverse transcript reagents (Takara Bio, Otsu, Japan). iQSYBR Green Supermix (Bio-Rad, Hercules, CA, USA) was used for real-time PCR (ABI Prime TM 7500 Sequence Detection System, PerkinElmer Applied Biosystems, Foster City, CA, USA). mRNA expression levels were quantified using the standard curve method, as reported previously [10]. Analytical data were adjusted, with the expression of GAPDH mRNA as the internal control. The following PCR primer sets were used: Drp1: forward, 5'-TCACCCGGAGACCTCTCATT-3′; reverse, 5'-TCTGCTTCCACCCCATTTTCT-3′,

OPA1: forward, 5'-AGTCATCGGTCAGACACCCTT-3′; reverse, 5'-GTGCAGCGTTATCTCCAACAG-3′, MFN2: forward, 5'-CTCTCGATGCAACTCTATCGTC-3′; reverse 5'-TCCTGTACGTGTCTTCAAGGAA-3′, MFN1: forward, 5'-TGGCTAAGAAGGCGATTACTGC-3′; reverse, 5'-CTCCGAGATAGCACCTCACC-3′, GAPDH: forward 5'-CAATGACCCCTTCATTGACC-3′; reverse 5'-GACAAGCTTCCCGTTCTCAG-3′.

2.10 Podocyte Preparation

Isolation of primary podocytes from *Drp1*$^{f/f}$ and Podo-*Drp1*$^{-/-}$ mice was performed as previously described with minor modifications [32, 33]. In brief, kidneys were dissected together with the abdominal aorta and transferred into dishes filled with 37°C-prewarmed PBS. Each kidney was slowly perfused through the renal artery with 1 ml of 37°C-prewarmed bead solution. Kidneys were minced and digested in a solution containing 300 U/ml collagenase (Worthington, Collagenase Type II, Lakewood, NJ), 1 mg/ml pronase E (Calbiochem, Darmstadt, Germany), and 50 U/ml DNase I (Takara Bio, Otsu, Japan). After several mechanical dissociation steps, the digested tissue slurry was inserted into a magnetic particle concentrator to separate glomeruli, which were washed twice. Isolated glomeruli were cultured on type I collagen-coated culture dishes in RPMI medium containing 5% fetal bovine serum supplemented with 0.5% Insulin–Transferrin–Selenium-A liquid media supplement (Invitrogen), 100 U/ml penicillin, and 100 µg/ml streptomycin. After isolated glomeruli were cultured for 4 days, subculture of primary podocytes was performed. Cellular outgrowths were detached with 0.05% trypsin solution and the remaining glomerular cores were removed with a magnetic separator. After washing with RPMI medium, cells were cultured on collagen I-coated dishes. Finally, cultured podocytes were stimulated with albumin under high-glucose condition, as described above.

2.11 Statistical analyses

Data are presented as mean ± standard error of the mean. Analysis of variance and Tukey's post-hoc test was used to determine significant differences between multiple groups. The Student's t-test was used for comparisons between two groups. $P<0.05$ was considered statistically significant.

Experimenters were not blinded to the treatment or genotypes of animals; however, semiquantitative analysis of renal histology was conducted blinded. Exclusion criteria were based on animal well-being at the beginning of the study. No animals were excluded from this study. No power analysis was performed to determine the sample size. The sample size in each study was based on experience with previous studies employing DKD animals and knockout mice in our lab.

3. RESULTS

3-1. Diabetic condition exacerbates podocyte damage under deficient endothelial glycocalyx.

First, we examined the association between albuminuria levels, loss of endothelial glycocalyx, and podocyte damage in STZ-induced diabetic mice. Compared with nondiabetic mice, at 3 weeks after STZ injection, diabetic mice developed significant but very mild albuminuria (Figure 1A), which was not accompanied by either loss of glycocalyx determined by isolectin staining or podocyte loss assessed by WT1-positive cell number in glomeruli (Figure 1 A–C). However, at 12 weeks after STZ injection, diabetic mice showed increased albuminuria with a decrease in isolectin-positive glycocalyx, and podocyte loss (Figure 1A–C), suggesting a pathological association between loss of glycocalyx, podocyte damage, and increased albuminuria during the progression of DKD in mice.

Neuraminidase administration-mediated glycocalyx removal can be used to cause transient mild albuminuria [12, 24, 25], therefore the effect of glycocalyx loss on podocyte damage under short-term diabetic condition (3 weeks) was tested using this experimental model (Figure 1D). At 3 weeks after induction of STZ-induced diabetes, blood glucose levels were significantly higher in diabetic mice (Figure 1E). On day 1 after neuraminidase administration, development of albuminuria was equivalent in both nondiabetic and diabetic mice (Figure 1F). Albuminuria recovered promptly in nondiabetic mice within 3 days after neuraminidase administration, whereas it remained elevated in diabetic mice at day 3 (Figure 1F). To examine the cause of persistent massive albuminuria in diabetic mice treated with neuraminidase, podocyte damage was examined. On day 1, no abnormalities in podocyte foot processes were observed in either nondiabetic or diabetic mice (Figure 1G), whereas on day 3, marked foot process alterations and significant decreases in podocyte number were observed in diabetic mice (Figure 1G and H).

3-2. High glucose inhibits albumin-induced mitochondrial elongation in podocytes.

Mitochondrial morphology in podocytes was examined using transmission electron microscopic analysis. The diabetic condition alone did not alter mitochondrial morphology in podocytes (Figure 2A and 2B). However, on day 1 after neuraminidase administration, mitochondrial length was significantly increased in podocytes from nondiabetic mice, while the diabetic condition prevented this change (Figure 2A and B). To identify factors associated with diabetes-related inhibition of mitochondrial elongation after neuraminidase administration, cell culture experiments were performed. Under normal glucose, albumin stimulation significantly increased mitochondrial length in cultured podocytes (Figure 2C and D). Among major pathogenic factors of DKD, including high glucose, TGF-β1, Ang-II, and TNF-α, only high glucose significantly inhibited albumin-induced mitochondrial elongation (Figure 2C and D). However, mannitol stimulation, as an osmotic control for high glucose, did not prevent albumin-induced mitochondrial elongation (Figure 2E and F).

3-3. High glucose inhibits albumin-induced decrease in Drp1 expression in podocytes. Mitochondrial dynamics are controlled by several proteins that regulate mitochondrial fusion and fission, such as Drp1, OPA1, Mfn1, and MFF [20], and therefore their gene expression levels were examined in cultured podocytes. Among these genes, only mRNA expression of Drp1, which promotes mitochondrial fission [20], was decreased by albumin stimulation (Figure 3A). Therefore, the effects of albumin and other stimuli associated with the pathogenesis of DKD on Drp1 protein expression levels were investigated. Consistent with the change in mRNA, albumin significantly decreased Drp1 protein expression levels, which was inhibited by co-stimulation with high glucose (Figure 3B). In contrast, other DKD-associated stimuli such as TGF-β1, Ang-II, and TNF-α did not alter albumin-induced decrease in Drp-1 protein expression (Figure 3B).

Drp1 expression in WT1-positive podocytes was decreased in nondiabetic mice administered neuraminidase, whereas diabetic condition abolished the effect on Drp1 expression in podocytes after neuraminidase treatment (Figure 3C). Furthermore, Drp1 expression increased in podocytes of mice at 12 weeks after STZ-mediated induction of diabetes, although the levels were not altered in podocytes of mice at 3 weeks after diabetes induction (Figure 3D).

3-4. High glucose exacerbates albumin-induced apoptosis in podocytes. Next, we examined the pathological significances of albumin- and high glucose-induced changes in mitochondrial morphology in cultured podocytes. Albumin-induced increase in cleaved caspase-3, a marker of apoptosis, was significantly enhanced under high glucose

condition (Figure 4A and B). The increase in apoptosis was accompanied by a significant decrease in intracellular ATP content in podocytes co-stimulated with albumin and high glucose (Figure 4C). Drp1 with a mutation in the 38th amino acid residue, from lysine to alanine (Drp1(K38A)), functions as a dominant-negative form of Drp1. Retroviral-mediated gene transfer of Drp1(K38A) in cultured podocytes promoted mitochondrial elongation even under coincubation with albumin and high glucose (Figure 4D and E). Furthermore, the Drp1 mutant prevented high glucose-induced increase in cleaved caspase-3 and ATP depletion in cultured podocytes co-stimulated with albumin and high glucose (Figure 4F and G).

3-5. Podocyte-specific Drp1 deficiency ameliorates podocyte damage in diabetic mice treated with neuraminidase. Taken together, our observations suggested the possibility of therapeutic Drp1 inhibition against albuminuria-associated podocyte damage in diabetes. To examine this possibility, tamoxifen-inducible Podo-*Drp1*$^{-/-}$ mice were generated by crossbreeding tamoxifen-inducible podocyte-specific Cre recombinase transgenic mice with Drp1-floxed (*Drp1*$^{f/f}$) mice (Figure 5A). Next, *Drp1*$^{f/f}$ and Podo-*Drp1*$^{-/-}$ mice were treated with/without STZ to induce diabetes, and neuraminidase was administrated after 3 weeks of STZ treatment (Figure 5A). Immunofluorescence analysis revealed diabetes-associated increase in Drp1 expression in podocytes after neuraminidase-induced glycocalyx removal, and complete deletion of Drp1 in podocytes from Podo-*Drp1*$^{-/-}$ mice (Figure 5B). Furthermore, after neuraminidase administration, mitochondrial length was decreased in podocytes in diabetic *Drp1*$^{f/f}$ mice treated with neuraminidase, which was prevented in Podo-*Drp1*$^{-/-}$ mice (Figure 5C and D). On days 0 and 1 after neuraminidase administration, urinary albumin excretion levels were consistent among all four groups of mice (Figure 5E). On day 2, non-diabetic *Drp1*$^{-/-}$ mice exhibited lower urinary excretion compared with *Drp1*$^{f/f}$ mice, however this difference was not statistically significant (Figure 5E). On day 3, urinary albumin excretion levels remained higher in diabetic *Drp1*$^{f/f}$ mice, whereas the levels were significantly lower in diabetic Podo-*Drp1*$^{-/-}$ mice (Figure 5E). Furthermore, podocyte-specific *Drp1*-deficiency prevented neuraminidase-induced alteration of podocyte foot processes and decrease in WT1-positive podocyte number under diabetic condition, although it did not alter diabetes-related glomerular hypertrophy (Figure 5F–H). In addition, the cleavage of caspase 3 observed following stimulation with albumin and high glucose in primary podocytes of *Drp1*$^{f/f}$ mice was not found in primary podocytes isolated from Podo-*Drp1*$^{-/-}$ mice (Figure 5I).

4. DISCUSSION

The present study confirmed that endothelial cell dysfunction-induced albumin exposure is cytotoxic for podocytes, and demonstrated that mitochondrial dynamics, notably inhibition of mitochondrial fission, is a cytoprotective mechanism against albumin exposure in podocytes under diabetes, although alteration of mitochondrial dynamics is not involved in normal podocyte development. Additionally, it was shown that diabetic condition, especially high glucose stimulation, suppressed cytoprotective inhibition of mitochondrial fission, leading to exacerbation of albumin-induced podocyte damage. Therefore, inhibition of mitochondrial fission may represent a promising therapeutic strategy in kidney diseases that involves endothelial dysfunction as an underlying pathogenic mechanism, including DKD.

The role of Drp1-mediated regulation of mitochondrial fission in diabetes-associated podocyte injury in db/db mice, an animal model of type 2 diabetes, was previously reported, in which inhibition of Drp1-related mitochondrial fission was renoprotective in DKD [34-36]. Other than these observations, there remains a lack of evidence that accurately demonstrates the significance of mitochondrial fission in podocytes in DKD using podocyte-specific gene-engineered mouse models. Our data show that inhibition of Drp1-related mitochondrial fission prevented podocyte damage under condition of STZ-induced type 1 diabetes, which is consistent with previous findings obtained from studies using db/db mice, and provide additional evidence that Drp1 inhibition may serve as a novel therapeutic intervention for DKD, regardless of type 1 or type 2 diabetes.

Acceleration of mitochondrial fission in podocytes has also been observed in human kidney biopsy samples [37]. Therefore, inhibition of mitochondrial fission may represent a potential therapeutic strategy for human DKD. However, details on how accelerated mitochondrial fission in podocytes in DKD contributes to deterioration of diabetes or kidney disease induced by various stimuli remain unclear. This study showed for the first time that inhibition of mitochondrial fission and promotion of mitochondrial fusion are cytoprotective mechanisms in podocytes when these cells are exposed to leaked albumin as a result of endothelial damage, and that high glucose-mediated impairment of this countermeasure against albumin triggers worsening podocyte damage and subsequent massive proteinuria.

Together with our previous finding that autophagy failure leads to worsening of albumin-induced podocyte damage in DKD, the present findings demonstrate that podocytes have several stress response mechanisms to cope with albumin-associated cytotoxicity, and their disruption contributes to worsening of podocyte damage, and

development of massive proteinuria in DKD. It has been suggested that there are individual differences in the degree of albuminuria (ranging from cases with only microalbuminuria to those with massive albuminuria) in DKD that cannot be explained by metabolic abnormalities alone. Genetic factors may certainly be involved as a cause of such individual differences [38], although our results also suggest the involvement of individual differences in the podocyte stress response mechanism to leaked albumin. The process of stage progression from endothelial damage to podocyte damage in DKD may involve a first hit of albumin efflux into podocytes via endothelial dysfunction and a second hit of disruption of the cellular stress response mechanism in podocytes. In addition to autophagy and mitochondrial dynamics, cells possess many other stress response mechanisms. On the basis of the two-hit theory in the pathogenesis of stage progression of DKD (albumin stimulation and altered cell protective machinery in podocytes), further exploration of stress response mechanisms in podocytes that permit them to cope with albumin-associated cytotoxicity may lead to elucidation of additional novel therapeutic targets for DKD.

Drp1 function has been reported to be primarily regulated by post-translational modifications such as phosphorylation, ubiquitination, and O-GlcNAcylation [20]. Additionally, altered expression levels of Drp1 is associated with pathological conditions in some disease models, ranging from cancer biology to metabolic diseases [39-42]. It was reported that hyperglycemia increases Drp1 expression, which is consistent with our findings. Furthermore, we found that stimulation with albumin decreased Drp1 expression as a protective mechanism in podocytes. As to whether this phenomenon is podocyte-specific or occurs in other cells, and if it occurs in numerous cell types, what the implications are, are interesting questions for the future because the endothelial glycocalyx is present in blood vessels throughout the body, and impaired glycocalyx function may be involved in damage of other organs in diabetes.

This study had limitations. Albumin stimulation decreased Drp1 expression, which was prevented under high glucose condition. The molecular mechanisms underlying changes in Drp1 expression levels in response to either albumin or high glucose have not been elucidated. Determination of these mechanisms may accelerate the development of drugs that modulate changes in Drp1 expression in DKD. Mitochondrial fission has been observed in human kidney biopsy samples [37], although it is unclear whether this was because of decreased expression of Drp1 protein, as observed in this study, or because of abnormalities in other mitochondrial dynamics-related proteins. Further examination will be required to confirm whether Drp1 can serve as a target for human DKD. The balance between mitochondrial fission and fusion is important for

maintaining cell function. In fact, Drp1 deficiency has been reported to be detrimental in the liver [43], so it is important to achieve a podocyte-specific or pathology-specific target for therapy. Lastly, neuraminidase was used to remove glomerular endothelial glycocalyx in this experiment. Although the significance of albumin stimulation for mitochondrial dynamics in podocytes was confirmed by experiments employing cultured cells, the effect of removing glycocalyx from podocytes and other renal cells cannot be completely ruled out in animal experiments using neuraminidase.

5. CONCLUSION

Podocytes are likely to have developed mechanisms that confer self-protection from albumin toxicity due to endothelial damage, and the mechanisms involve mitochondrial dynamics. Amelioration of abnormal mitochondrial dynamics via regulation of Drp1 function may become a promising treatment strategy for preventing stage progression of albuminuria in DKD.

CRediT authorship contribution statement

M.T. designed the study, performed experiments, analyzed data, and wrote the manuscript; S.K. designed the study, analyzed data, and wrote the manuscript; M.Y.-Y. and Y.N. performed experiments. S.K., K.Y., N.T., and M.C.-K. interpreted data and edited the manuscript; K.M. and S.-i. A. supervised the study, analyzed and interpreted data, and critically reviewed and edited the manuscript. H.Y., M.M., N.I., and M.N generated animal models. All the authors have approved the final version of this manuscript. KS. and ASi are the guarantors of this work.

Declaration of competing interest

The authors declare that there are no relationships or activities that might bias, or be perceived to bias, their work.

Acknowledgements

We thank Naoko Yamanaka and Keiko Kosaka (Shiga University of Medical Science) and the Central Research Laboratory of Shiga University of Medical Science for their technical assistance.

Funding
This study was partly supported by a research grant from Boehringer Ingelheim, Daiichi Sankyo, and Torii Pharmaceutical.

REFERENCES

[1] A.S. Krolewski, Progressive renal decline: the new paradigm of diabetic nephropathy in type 1 diabetes, Diabetes Care, 38 (2015) 954-962.
[2] A.S. Krolewski, J. Skupien, P. Rossing, J.H. Warram, Fast renal decline to end-stage renal disease: an unrecognized feature of nephropathy in diabetes, Kidney Int, 91 (2017) 1300-1311.
[3] M. Brownlee, Biochemistry and molecular cell biology of diabetic complications, Nature, 414 (2001) 813-820.
[4] M. Brownlee, The pathobiology of diabetic complications: a unifying mechanism, Diabetes, 54 (2005) 1615-1625.
[5] K.E. White, R.W. Bilous, S.M. Marshall, M. El Nahas, G. Remuzzi, G. Piras, S. De Cosmo, G. Viberti, Podocyte number in normotensive type 1 diabetic patients with albuminuria, Diabetes, 51 (2002) 3083-3089.
[6] M.E. Pagtalunan, P.L. Miller, S. Jumping-Eagle, R.G. Nelson, B.D. Myers, H.G. Rennke, N.S. Coplon, L. Sun, T.W. Meyer, Podocyte loss and progressive glomerular injury in type II diabetes, J Clin Invest, 99 (1997) 342-348.
[7] N. Jourde-Chiche, F. Fakhouri, L. Dou, J. Bellien, S. Burtey, M. Frimat, P.A. Jarrot, G. Kaplanski, M. Le Quintrec, V. Pernin, C. Rigothier, M. Sallée, V. Fremeaux-Bacchi, D. Guerrot, L.T. Roumenina, Endothelium structure and function in kidney health and disease, Nat Rev Nephrol, 15 (2019) 87-108.
[8] T.J. Rabelink, D. de Zeeuw, The glycocalyx--linking albuminuria with renal and cardiovascular disease, Nat Rev Nephrol, 11 (2015) 667-676.
[9] B.M. van den Berg, G. Wang, M.G.S. Boels, M.C. Avramut, E. Jansen, W.M.P.J. Sol, F. Lebrin, A.J. van Zonneveld, E.J.P. de Koning, H. Vink, H.J. Gröne, P. Carmeliet, J. van der Vlag, T.J. Rabelink, Glomerular Function and Structural Integrity Depend on Hyaluronan Synthesis by Glomerular Endothelium, J Am Soc Nephrol, 30 (2019) 1886-1897.
[10] K. Yamahara, S. Kume, D. Koya, Y. Tanaka, Y. Morita, M. Chin-Kanasaki, H. Araki, K. Isshiki, S. Araki, M. Haneda, T. Matsusaka, A. Kashiwagi, H. Maegawa, T. Uzu, Obesity-mediated autophagy insufficiency exacerbates proteinuria-induced tubulointerstitial lesions, J Am Soc Nephrol, 24 (2013) 1769-1781.

[11] A. Kamijo, K. Kimura, T. Sugaya, M. Yamanouchi, H. Hase, T. Kaneko, Y. Hirata, A. Goto, T. Fujita, M. Omata, Urinary free fatty acids bound to albumin aggravate tubulointerstitial damage, Kidney Int, 62 (2002) 1628-1637.
[12] M. Yoshibayashi, S. Kume, M. Yasuda-Yamahara, K. Yamahara, N. Takeda, N. Osawa, M. Chin-Kanasaki, Y. Nakae, H. Yokoi, M. Mukoyama, K. Asanuma, H. Maegawa, S.I. Araki, Protective role of podocyte autophagy against glomerular endothelial dysfunction in diabetes, Biochem Biophys Res Commun, 525 (2020) 319-325.
[13] S. Agrawal, A.J. Guess, M.A. Chanley, W.E. Smoyer, Albumin-induced podocyte injury and protection are associated with regulation of COX-2, Kidney Int, 86 (2014) 1150-1160.
[14] F. He, S. Chen, H. Wang, N. Shao, X. Tian, H. Jiang, J. Liu, Z. Zhu, X. Meng, C. Zhang, Regulation of CD2-associated protein influences podocyte endoplasmic reticulum stress-mediated apoptosis induced by albumin overload, Gene, 484 (2011) 18-25.
[15] K. Okamura, P. Dummer, J. Kopp, L. Qiu, M. Levi, S. Faubel, J. Blaine, Endocytosis of albumin by podocytes elicits an inflammatory response and induces apoptotic cell death, PLoS One, 8 (2013) e54817.
[16] N. Mizushima, B. Levine, Autophagy in Human Diseases, N Engl J Med, 383 (2020) 1564-1576.
[17] N. Mizushima, M. Komatsu, Autophagy: renovation of cells and tissues, Cell, 147 (2011) 728-741.
[18] S. Ueda, S. Ozawa, K. Mori, K. Asanuma, M. Yanagita, S. Uchida, T. Nakagawa, ENOS deficiency causes podocyte injury with mitochondrial abnormality, Free Radic Biol Med, 87 (2015) 181-192.
[19] J. Su, D. Ye, C. Gao, Q. Huang, D. Gui, Mechanism of progression of diabetic kidney disease mediated by podocyte mitochondrial injury, Mol Biol Rep, 47 (2020) 8023-8035.
[20] H. Otera, N. Ishihara, K. Mihara, New insights into the function and regulation of mitochondrial fission, Biochim Biophys Acta, 1833 (2013) 1256-1268.
[21] L. Wang, T. Ishihara, Y. Ibayashi, K. Tatsushima, D. Setoyama, Y. Hanada, Y. Takeichi, S. Sakamoto, S. Yokota, K. Mihara, D. Kang, N. Ishihara, R. Takayanagi, M. Nomura, Disruption of mitochondrial fission in the liver protects mice from diet-induced obesity and metabolic deterioration, Diabetologia, 58 (2015) 2371-2380.
[22] T.G. Hennings, D.G. Chopra, E.R. DeLeon, H.R. VanDeusen, H. Sesaki, M.J. Merrins, G.M. Ku, In Vivo Deletion of β-Cell Drp1 Impairs Insulin Secretion Without Affecting Islet Oxygen Consumption, Endocrinology, 159 (2018) 3245-3256.
[23] F.C. Brosius, C.E. Alpers, E.P. Bottinger, M.D. Breyer, T.M. Coffman, S.B. Gurley,

R.C. Harris, M. Kakoki, M. Kretzler, E.H. Leiter, M. Levi, R.A. McIndoe, K. Sharma, O. Smithies, K. Susztak, N. Takahashi, T. Takahashi, A.M.o.D.C. Consortium, Mouse models of diabetic nephropathy, J Am Soc Nephrol, 20 (2009) 2503-2512.
[24] A.H. Salmon, J.K. Ferguson, J.L. Burford, H. Gevorgyan, D. Nakano, S.J. Harper, D.O. Bates, J. Peti-Peterdi, Loss of the endothelial glycocalyx links albuminuria and vascular dysfunction, J Am Soc Nephrol, 23 (2012) 1339-1350.
[25] K.B. Betteridge, K.P. Arkill, C.R. Neal, S.J. Harper, R.R. Foster, S.C. Satchell, D.O. Bates, A.H.J. Salmon, Sialic acids regulate microvessel permeability, revealed by novel in vivo studies of endothelial glycocalyx structure and function, J Physiol, 595 (2017) 5015-5035.
[26] N. Ishihara, M. Nomura, A. Jofuku, H. Kato, S.O. Suzuki, K. Masuda, H. Otera, Y. Nakanishi, I. Nonaka, Y. Goto, N. Taguchi, H. Morinaga, M. Maeda, R. Takayanagi, S. Yokota, K. Mihara, Mitochondrial fission factor Drp1 is essential for embryonic development and synapse formation in mice, Nat Cell Biol, 11 (2009) 958-966.
[27] H. Yokoi, M. Kasahara, M. Mukoyama, K. Mori, K. Kuwahara, J. Fujikura, Y. Arai, Y. Saito, Y. Ogawa, T. Kuwabara, A. Sugawara, K. Nakao, Podocyte-specific expression of tamoxifen-inducible Cre recombinase in mice, Nephrol Dial Transplant, 25 (2010) 2120-2124.
[28] S. Ono, S. Kume, M. Yasuda-Yamahara, K. Yamahara, N. Takeda, M. Chin-Kanasaki, H. Araki, O. Sekine, H. Yokoi, M. Mukoyama, T. Uzu, S.I. Araki, H. Maegawa, O-linked β-N-acetylglucosamine modification of proteins is essential for foot process maturation and survival in podocytes, Nephrol Dial Transplant, 32 (2017) 1477-1487.
[29] M.A. Saleem, M.J. O'Hare, J. Reiser, R.J. Coward, C.D. Inward, T. Farren, C.Y. Xing, L. Ni, P.W. Mathieson, P. Mundel, A conditionally immortalized human podocyte cell line demonstrating nephrin and podocin expression, J Am Soc Nephrol, 13 (2002) 630-638.
[30] M. Yasuda, Y. Tanaka, S. Kume, Y. Morita, M. Chin-Kanasaki, H. Araki, K. Isshiki, S. Araki, D. Koya, M. Haneda, A. Kashiwagi, H. Maegawa, T. Uzu, Fatty acids are novel nutrient factors to regulate mTORC1 lysosomal localization and apoptosis in podocytes, Biochim Biophys Acta, 1842 (2014) 1097-1108.
[31] S. Kume, M. Haneda, K. Kanasaki, T. Sugimoto, S. Araki, K. Isshiki, M. Isono, T. Uzu, L. Guarente, A. Kashiwagi, D. Koya, SIRT1 inhibits transforming growth factor beta-induced apoptosis in glomerular mesangial cells via Smad7 deacetylation, J Biol Chem, 282 (2007) 151-158.
[32] C. Schell, B. Sabass, M. Helmstaedter, F. Geist, A. Abed, M. Yasuda-Yamahara, A. Sigle, J.I. Maier, F. Grahammer, F. Siegerist, N. Artelt, N. Endlich, D. Kerjaschki, H.H. Arnold, J. Dengjel, M. Rogg, T.B. Huber, ARP3 Controls the Podocyte Architecture at

the Kidney Filtration Barrier, Dev Cell, 47 (2018) 741-757.e748.
[33] K. Katsuya, E. Yaoita, Y. Yoshida, Y. Yamamoto, T. Yamamoto, An improved method for primary culture of rat podocytes, Kidney Int, 69 (2006) 2101-2106.
[34] W. Wang, Y. Wang, J. Long, J. Wang, S.B. Haudek, P. Overbeek, B.H. Chang, P.T. Schumacker, F.R. Danesh, Mitochondrial fission triggered by hyperglycemia is mediated by ROCK1 activation in podocytes and endothelial cells, Cell Metab, 15 (2012) 186-200.
[35] B.A. Ayanga, S.S. Badal, Y. Wang, D.L. Galvan, B.H. Chang, P.T. Schumacker, F.R. Danesh, Dynamin-Related Protein 1 Deficiency Improves Mitochondrial Fitness and Protects against Progression of Diabetic Nephropathy, J Am Soc Nephrol, 27 (2016) 2733-2747.
[36] D.L. Galvan, J. Long, N. Green, B.H. Chang, J.S. Lin, P. Schumacker, L.D. Truong, P. Overbeek, F.R. Danesh, Drp1S600 phosphorylation regulates mitochondrial fission and progression of nephropathy in diabetic mice, J Clin Invest, 129 (2019) 2807-2823.
[37] Y. Ma, Z. Chen, Y. Tao, J. Zhu, H. Yang, W. Liang, G. Ding, Increased mitochondrial fission of glomerular podocytes in diabetic nephropathy, Endocr Connect, 8 (2019) 1206-1212.
[38] S. Maeda, Genome-wide search for susceptibility gene to diabetic nephropathy by gene-based SNP, Diabetes Res Clin Pract, 66 Suppl 1 (2004) S45-47.
[39] L. Zhang, X. Gan, Y. He, Z. Zhu, J. Zhu, H. Yu, Drp1-dependent mitochondrial fission mediates osteogenic dysfunction in inflammation through elevated production of reactive oxygen species, PLoS One, 12 (2017) e0175262.
[40] D.B. Wang, G.A. Garden, C. Kinoshita, C. Wyles, N. Babazadeh, B. Sopher, Y. Kinoshita, R.S. Morrison, Declines in Drp1 and parkin expression underlie DNA damage-induced changes in mitochondrial length and neuronal death, J Neurosci, 33 (2013) 1357-1365.
[41] J. Liu, Z. Chen, Y. Zhang, M. Zhang, X. Zhu, Y. Fan, S. Shi, K. Zen, Z. Liu, Rhein protects pancreatic β-cells from dynamin-related protein-1-mediated mitochondrial fission and cell apoptosis under hyperglycemia, Diabetes, 62 (2013) 3927-3935.
[42] A. Ferreira-da-Silva, C. Valacca, E. Rios, H. Pópulo, P. Soares, M. Sobrinho-Simões, L. Scorrano, V. Máximo, S. Campello, Mitochondrial dynamics protein Drp1 is overexpressed in oncocytic thyroid tumors and regulates cancer cell migration, PLoS One, 10 (2015) e0122308.
[43] L. Wang, X. Li, Y. Hanada, N. Hasuzawa, Y. Moriyama, M. Nomura, K. Yamamoto, Dynamin-related protein 1 deficiency accelerates lipopolysaccharide-induced acute liver injury and inflammation in mice, Commun Biol, 4 (2021) 894.

FIGURE LEGENDS

Figure 1. Loss of glomerular endothelial glycocalyx causes podocyte injury in diabetic mice. (A) Urinary albumin excretion in nondiabetic mice at 3 weeks after vehicle administration (nonDM, n = 13), and streptozotocin (STZ)-induced diabetic mice (DM) at 3 weeks (n = 10) and 12 weeks (n = 8) after STZ administration. (B) Isolectin and WT1 stains to assess endothelial glycocalyx expression and podocyte number, respectively. DAPI stain was used to visualize nuclei. (C) WT1-positive cell count to assess podocyte number in glomeruli. (D) Study protocol to examine the effect of DM on podocyte damage in mice injected with neuraminidase to pharmacologically remove glomerular endothelial glycocalyx (n = 8 mice per group). (E) Fasting blood glucose levels at 3 weeks after STZ injection. (F) Time-dependent change in urinary albumin excretion levels after neuraminidase injection in nonDM and DM mice. (G) Scanning electron microscopic (SEM) analysis of podocytes under the indicated conditions. (H) Representative pictures for WT1 immunofluorescent study. WT1-positive podocyte number in nonDM and DM mice at day 3 after neuraminidase injection. Data are presented as mean ± standard error of the mean. NS: not significant.

Figure 2. High glucose condition inhibits albumin-induced mitochondrial elongation. (A) Representative transmission electron microscopic images of podocytes of the indicated four groups of mice. The area circled in red in the lower panel is for visualizing the mitochondrial region in the upper panel. (B) The length of the long axis of the enclosed region in Figure 2A was defined as the mitochondrial length, which was quantitatively evaluated in nondiabetic (nonDM) and diabetic (DM) mice treated with/without neuraminidase (Neu). (C) The effect of albumin stimulation on mitochondrial length in cultured podocytes under either normal glucose (NG) condition or stimulated with high glucose (HG), TGF-β1, angiotensin II (Ang-II), or TNF-α. (D) Quantitative data for mitochondrial length under the indicated conditions. (E) Effects of HG+albumin and mannitol+albumin on mitochondrial length in cultured podocytes. (F) Quantitative data for mitochondrial length under the indicated conditions. Data are presented as mean ± standard error of the mean. NS: not significant.

Figure 3. High glucose condition inhibits albumin-induced reduction of Drp1 expression. (A) mRNA expression levels of Drp1, OPA1, Mfn1, MFF, which are all involved in mitochondria fission and fusion. (B) Representative figures and quantitative analysis of immunoblot of Drp1 in the cultured podocytes under normal condition or stimulated with high glucose (HG) TGF-β1, angiotensin II (Ang-II) or TNF-α. β actin

was used as an internal control. (C) Representative pictures for WT1 and Drp1 double immunofluorescent stains in the kidney of nonDM and DM mice at day 3 after the neuraminidase injection. (D) Representative pictures for WT1 and Drp1 double immunofluorescent study in the kidneys of non-diabetic (nonDM) and diabetic (DM) mice at the indicated weeks after streptozotocin (STZ) administration. The results are presented as mean ± SEM. NS: not significant.

Figure 4. Inhibition of Drp1 prevents apoptosis and ATP depletion in cultured podocytes costimulated with albumin and high glucose. (A) Immunoblots of cleaved caspase-3 in cultured podocytes stimulated with/without albumin under normal glucose (NG) and high glucose (HG) conditions. β-actin was used as the internal control. (B) Quantitative analysis of the ratio of cleaved caspase-3 to β-actin. (C) Intracellular ATP content under the indicated conditions. (D) Representative images of MitoTracker Red-stained podocytes retrovirally transduced with the dominant-negative form of Drp1 (Drp1(K38A)) or nontransduced (Empty). (E) Quantitative analysis of mitochondrial length. (F, G) Representative images (F) and quantitative analysis (G) of immunoblots of cleaved caspase-3 under the indicated conditions. (H) Intracellular ATP content under the indicated conditions. Data are presented as mean ± standard error of the mean. NS: not significant.

Figure 5. Podocyte-specific Drp1 deficiency prevents progression of albuminuria and podocyte damage in diabetic mice. (A) Study protocol to examine the effect of podocyte-specific Drp1 deficiency in neuraminidase-induced albuminuria development under diabetic condition. Numbers of mice used in this study are shown in the figure. (B) Representative pictures for WT1 and Drp1 double immunofluorescent stains in the kidneys of non-diabetic *Drp1*-flox mice (nonDM-*Drp1*$^{f/f}$), diabetic Drp1-flox mice (DM-*Drp1*$^{f/f}$), non-diabetic podocyte-specific Drp1-deficient mice (nonDM-Podo-*Drp1*$^{-/-}$) and diabetic podocyte-specific Drp1-deficient mice (DM-Podo-*Drp1*$^{-/-}$). (C) Representative pictures of transmission electron microscopy of podocytes. Mitochondria area was marked with red-colored line. (D) The length of the long axis of the enclosed region in figure 5C was defined as the length of the mitochondria, and the length of mitochondria was quantitatively evaluated in the indicated groups of mice. (E) Time-dependent change in urinary albumin excretion levels after the neuraminidase injection in the four groups of mice. (F) Representative pictures for scanning electron microscopic (SEM) analysis of podocytes and WT1 immunofluorescent study at the indicated groups. (G) WT1-positive podocyte number in the indicated groups of mice at day 3 after the neuraminidase

injection. (H) Glomerular size in the indicated groups of mice. (I) Expression levels of Drp1 and cleaved caspase 3 in primary podocytes isolated from nonDM-*Drp1*$^{f/f}$ mice and nonDM-Podo-*Drp1*$^{-/-}$ mice, which were cultured under high glucose (HG) and albumin stimulation. The results are presented as mean ± SEM. NS: not significant.

Figure 1

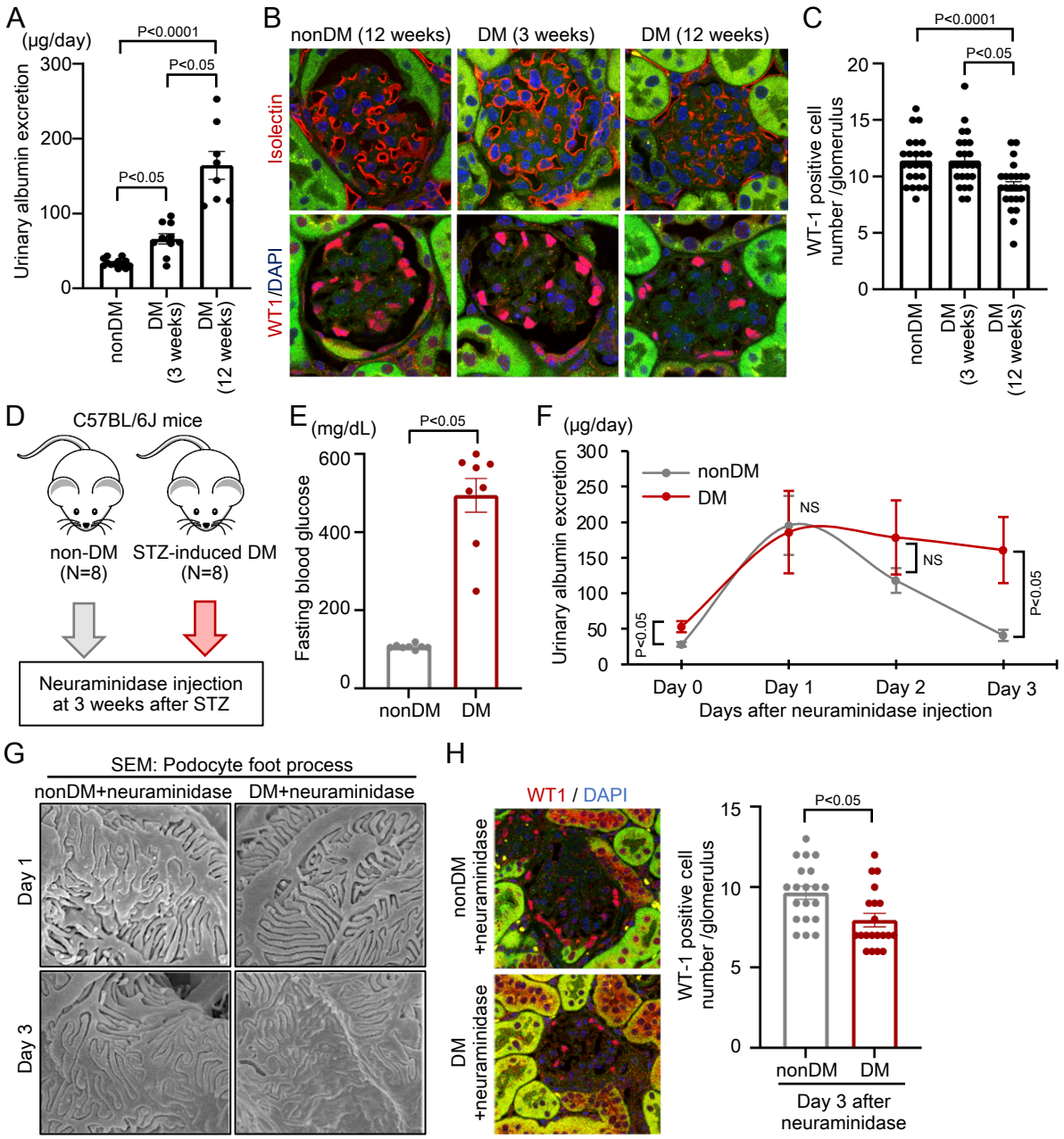
A
(μg/day)
Urinary albumin excretion
300
200
100
0
P<0.0001
P<0.05
P<0.05
nonDM
DM (3 weeks)
DM (12 weeks)
B
nonDM (12 weeks)
DM (3 weeks)
DM (12 weeks)
Isolectin
WT1/DAPI
C
P<0.0001
P<0.05
WT-1 positive cell number /glomerulus
20
15
10
5
0
nonDM
DM (3 weeks)
DM (12 weeks)
D
C57BL/6J mice
non-DM (N=8)
STZ-induced DM (N=8)
Neuraminidase injection at 3 weeks after STZ
E
(mg/dL)
P<0.05
Fasting blood glucose
600
400
200
0
nonDM
DM
F
(μg/day)
Urinary albumin excretion
300
250
200
150
100
50
0
nonDM
DM
NS
NS
P<0.05
P<0.05
Day 0
Day 1
Day 2
Day 3
Days after neuraminidase injection
G
SEM: Podocyte foot process
nonDM+neuraminidase
DM+neuraminidase
Day 1
Day 3
H
WT1 / DAPI
nonDM +neuraminidase
DM +neuraminidase
P<0.05
WT-1 positive cell number /glomerulus
15
10
5
0
nonDM
DM
Day 3 after neuraminidase

Figure 2

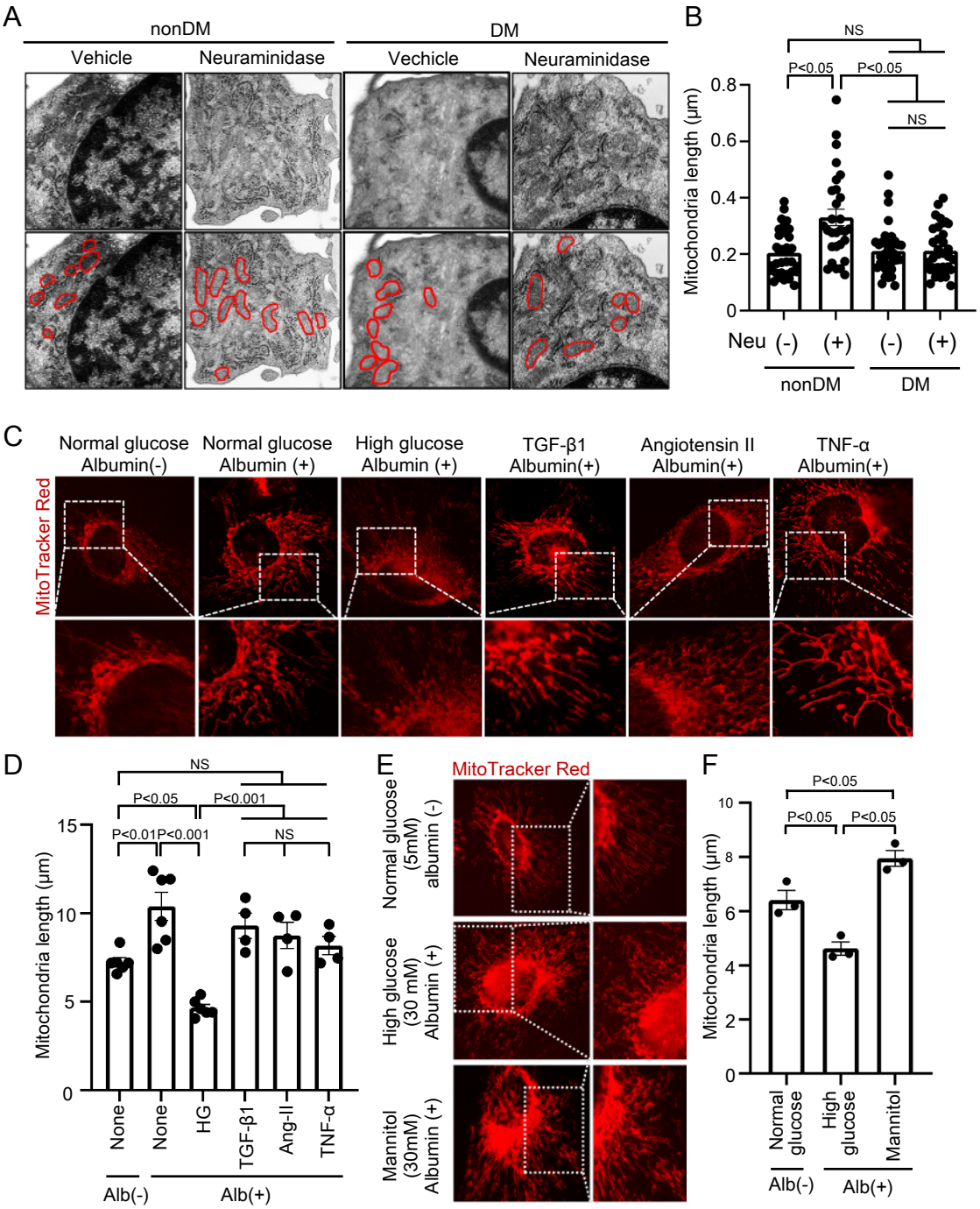
A
nonDM
DM
Vehicle
Neuraminidase
Vechicle
Neuraminidase
B
NS
P<0.05
P<0.05
NS
Mitochondria length (μm)
0.8
0.6
0.4
0.2
0
Neu (-) (+) (-) (+)
nonDM
DM
C
Normal glucose Albumin(-)
Normal glucose Albumin (+)
High glucose Albumin (+)
TGF-β1 Albumin(+)
Angiotensin II Albumin(+)
TNF-α Albumin(+)
MitoTracker Red
D
NS
P<0.05
P<0.001
P<0.01
P<0.001
NS
Mitochondria length (μm)
15
10
5
0
None
None
HG
TGF-β1
Ang-II
TNF-α
Alb(-)
Alb(+)
E
MitoTracker Red
Normal glucose (5mM) albumin (-)
High glucose (30 mM) Albumin (+)
Mannitol (30mM) Albumin (+)
F
P<0.05
P<0.05
P<0.05
Mitochondria length (μm)
10
8
6
4
2
0
Normal glucose
High glucose
Mannitol
Alb(-)
Alb(+)

Figure 3

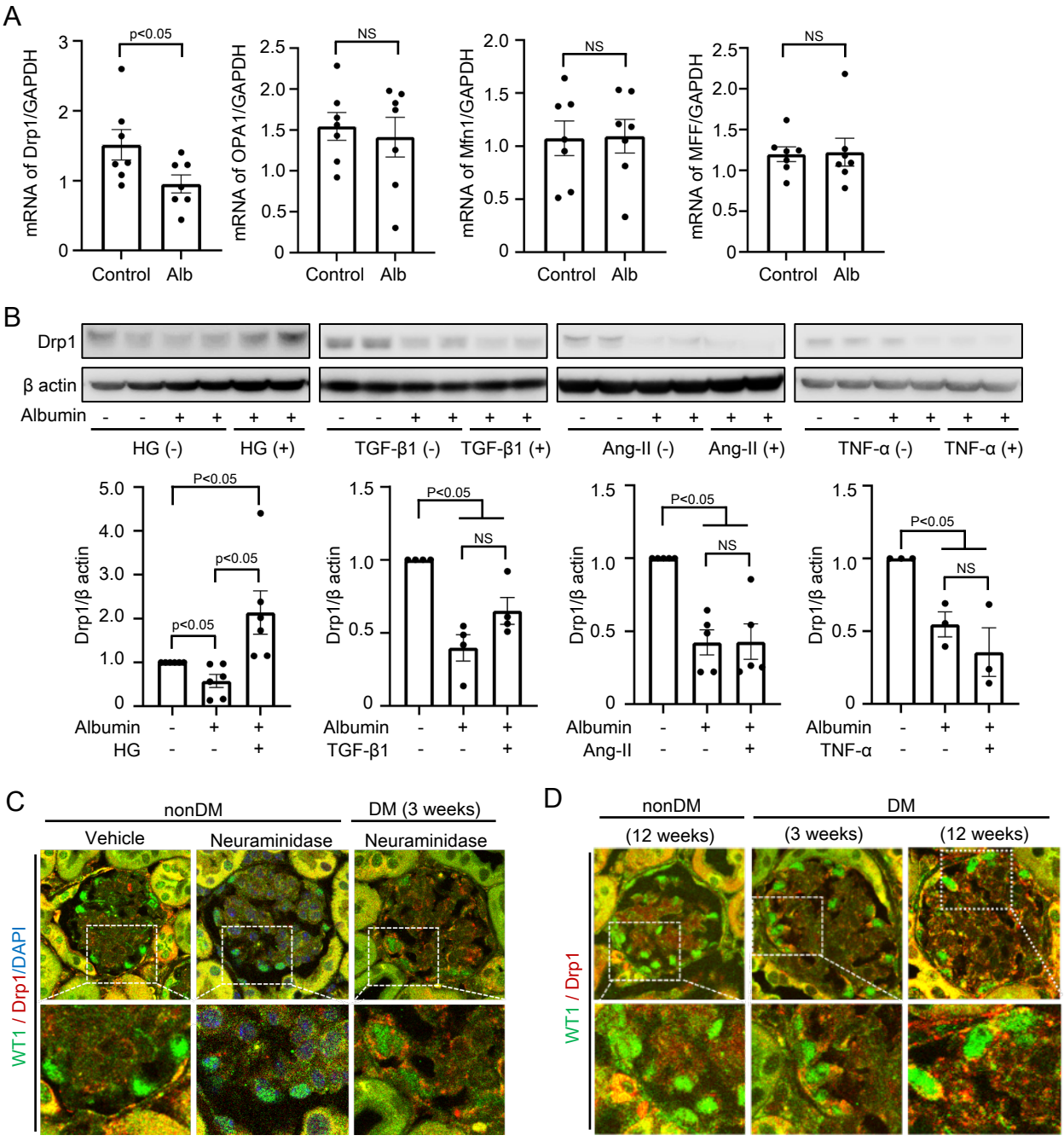
A
mRNA of Drp1/GAPDH
p<0.05
Control
Alb
mRNA of OPA1/GAPDH
NS
mRNA of Mfn1/GAPDH
mRNA of MFF/GAPDH
B
Drp1
β actin
Albumin
HG (-)
HG (+)
TGF-β1 (-)
TGF-β1 (+)
Ang-II (-)
Ang-II (+)
TNF-α (-)
TNF-α (+)
Drp1/β actin
P<0.05
HG
TGF-β1
Ang-II
TNF-α
C
nonDM
DM (3 weeks)
Vehicle
Neuraminidase
WT1 / Drp1/DAPI
D
DM
(12 weeks)
(3 weeks)
WT1 / Drp1

Figure 4

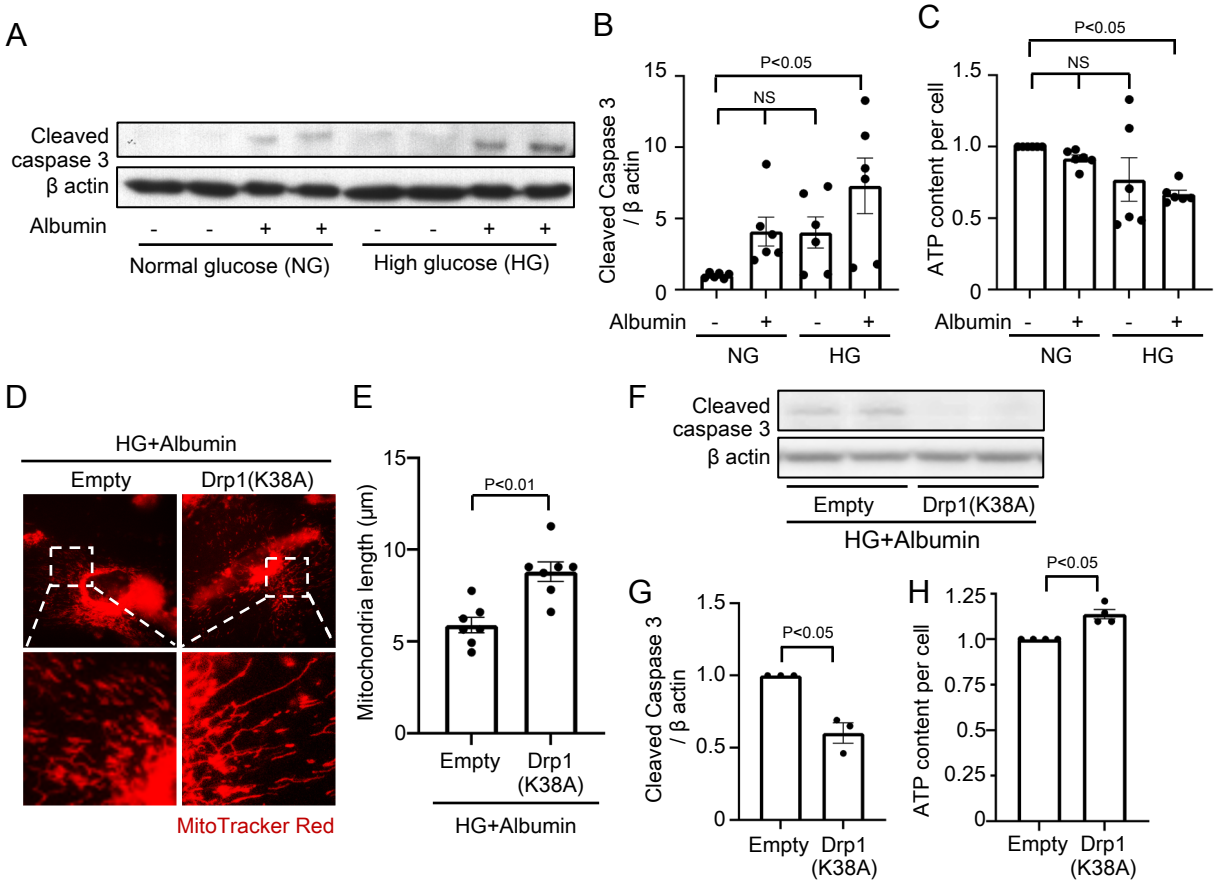
A
Cleaved caspase 3
β actin
Albumin
- - + + - - + +
Normal glucose (NG)
High glucose (HG)
B
Cleaved Caspase 3 / β actin
P<0.05
NS
Albumin - + - +
NG
HG
C
ATP content per cell
P<0.05
NS
Albumin - + - +
NG
HG
D
HG+Albumin
Empty
Drp1(K38A)
MitoTracker Red
E
Mitochondria length (μm)
P<0.01
Empty
Drp1 (K38A)
HG+Albumin
F
Cleaved caspase 3
β actin
Empty
Drp1(K38A)
HG+Albumin
G
Cleaved Caspase 3 / β actin
P<0.05
Empty
Drp1 (K38A)
H
ATP content per cell
P<0.05
Empty
Drp1 (K38A)

Figure 5

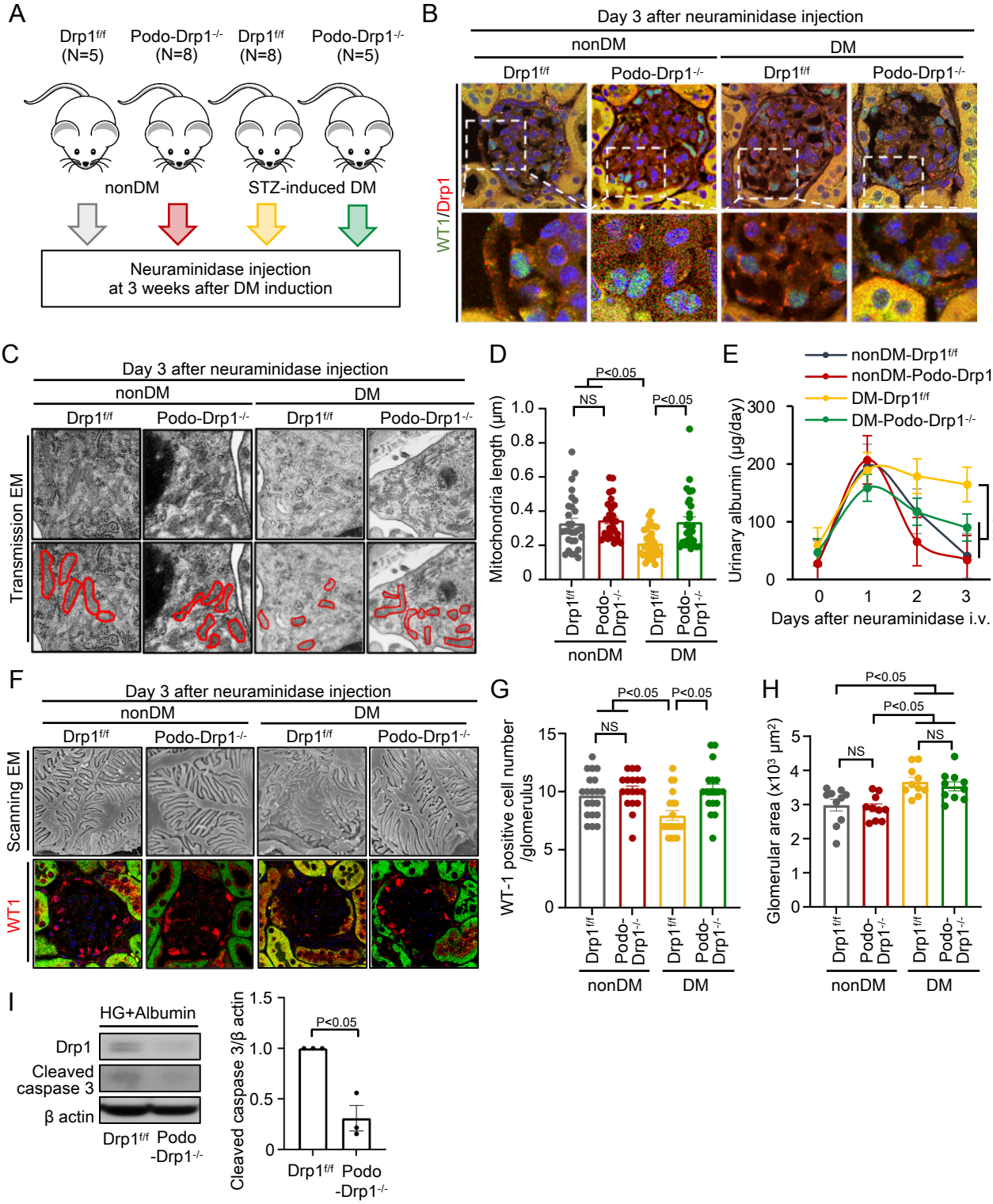
A
Drp1f/f (N=5)
Podo-Drp1-/- (N=8)
Drp1f/f (N=8)
Podo-Drp1-/- (N=5)
nonDM
STZ-induced DM
Neuraminidase injection at 3 weeks after DM induction
B
Day 3 after neuraminidase injection
nonDM
DM
Drp1f/f
Podo-Drp1-/-
WT1/Drp1
C
Day 3 after neuraminidase injection
Transmission EM
D
Mitochondria length (μm)
P<0.05
NS
E
nonDM-Drp1f/f
nonDM-Podo-Drp1-/-
DM-Drp1f/f
DM-Podo-Drp1-/-
Urinary albumin (μg/day)
Days after neuraminidase i.v.
F
Scanning EM
WT1
G
WT-1 positive cell number /glomerulus
H
Glomerular area (x10³ μm²)
I
HG+Albumin
Drp1
Cleaved caspase 3
β actin
Cleaved caspase 3/β actin